Am J Transl Res 2021;13(12):13438-13451
www.ajtr.org /ISSN:1943-8141/AJTR0132208

Original Article

Effect of tissue expansion on chondrocyte sheets in cartilage composite reconstruction

Chu-Hsin Chen, Peng Xu, Yahong Chen, Ke Xue, Kai Liu

Department of Plastic and Reconstructive Surgery, Shanghai Ninth People's Hospital, Shanghai Jiao Tong University School of Medicine, 639 Zhi Zao Ju Road, Shanghai 200011, People's Republic of China

Received February 21, 2021; Accepted October 26, 2021; Epub December 15, 2021; Published December 30, 2021

Abstract: Flap prelamination has been successfully established in tissue engineering; however, cartilage generation through combination of an expanded flap and chondrocyte sheets has not been reported. Herein, we investigate the effect of tissue expansion on chondrocyte sheets in prelaminating an expanded chondrocutaneous flap. Chondrocyte sheets were implanted into a tissue expander capsule following which capsule inflation was performed weekly. At 4 and 12 weeks post implantation, the specimens were examined with histology and immunohistochemistry analyses. Extracellular matrix (ECM) formation and type II collagen deposition in the regenerated cartilage tissue *in vivo* were also examined. After 4 weeks of implantation, the generated cartilage was phenotypically stable with minimal hypertrophy, while that formed after the 12-week expansion showed visible hypertrophic differentiation. To evaluate the effect of static pressure and/or hypoxic conditions generated by the expanding tissue, static pressure and/or hypoxic conditions were reproduced *in vitro*. The chondrocyte sheets stimulated by mechanical static pressure and hypoxia maintained their chondrogenic phenotype. The expression of aggrecan, collagen II, Sox-9, and HIF-1α was increased in chondrocyte sheets cultured in 2% oxygen (hypoxia); however, aggrecan, collagen II, and Sox-9 were downregulated in the static pressure/normoxia group. These results suggest that the expanded environment promoted cartilage formation by the chondrocyte cell sheets, while mechanical forces and hypoxic conditions *in vitro* allowed chondrocyte cell sheets to retain their chondrogenic phenotype.

Keywords: Cell sheet, chondrocyte, prelamination, tissue expansion, chondrocutaneous flap

Introduction

In reconstructive surgeries, especially those performed for complex tissue defects caused by trauma, burns, or tumor resection, tissue flaps are commonly used [1]. This method requires a combination of different tissues, including cartilage, bone, skin, muscle, and fascia. Certain anatomic prerequisites must also be fulfilled to harvest a suitable free flap. One promising approach, flap prefabrication, allows for the creation of axial perfused flaps for transposition or microvascular transfer [2]. The term "prefabrication" was first introduced by Yao *et al*. [3] to describe the implantation of a vascular pedicle under a skin flap. Pribaz *et al*. [4] later defined "prelamination", which includes additional modifications to the flap without manipulating the blood supply, thereby allowing for the customization of flaps for various recipient sites. Using tissue expansion, an important technique widely applied in plastic and reconstructive surgeries [5, 6], the color, thickness, and texture of the expanded skin can be matched to the defect area. Mutaf *et al*. [7] indicated that skin expansion creates a favorable environment for cartilage grafting and reported the growth potential of the cartilage framework. The integration of a second tissue component, such as cartilage, into a free flap can provide shape and stability. Thus, the reconstruction of complex three-dimensional areas is possible even under unfavorable conditions.

Although autologous tissue harvesting has been shown to cause donor-site morbidity [8], tissue engineering of cartilage can create a new possibility for reconstructive surgery. Staudenmaier *et al*. [9] have reported the benefits of prelaminating prefabricated flaps with tissue-engineered cartilage, generating a functional composite tissue while minimizing donor-

site morbidity. Conventional tissue engineering with scaffold-seeded cells is associated with a high rate of cell death or loss primarily due to graft site mechanical injury and inflammation [10]. To overcome these limitations, the scaffold-free cell sheet technique has recently been proposed, which generates autologous cell sheets without foreign materials, thereby eliminating inflammation and the risk associated with immune rejection [11].

Soft tissue expansion is associated with the irritation of the expander and relative mechanical forces, transient ischemia, and hypoxia due to an increase in vascularity [12, 13]. At the same time, the application of mechanical pressure on chondrocytes creates a balance between cell proliferation and apoptosis, reduces necrosis, and promotes chondrogenesis and chondrocyte hypertrophy [14]. Li *et al*. [15] have demonstrated that the HIF-1α/YAP signaling axis is involved in the regulation of chondrocyte differentiation and the maintenance of chondrogenic phenotype in these cells.

We hypothesize that the tissue expander provides mechanical and hypoxic stresses to maintain the chondrocyte phenotype. To test our hypothesis, we have evaluated the effect of tissue expansion on chondrocyte sheets during the prelamination of expanded chondrocutaneous flap with chondrocyte sheets. Chondrocyte sheets were characterized and the expression of aggrecan, collagen II, Sox-9, and HIF-1α was determined under static pressure and hypoxic stimulation *in vitro*.

Materials and methods

In vitro chondrocyte isolation, culture, and identification

Isolation of chondrocytes: All procedures performed in this study were approved by the Research Ethics Committee of Shanghai Ninth People's Hospital (approval number: SH9H-2019-T261-1). Primary chondrocytes were isolated from knee joints of one-week-old Sprague-Dawley rats. The articular cartilage was cut into pieces (1-2 mm^3) and digested with 2% type II collagenase (Sigma-Aldrich, St. Louis, MO, USA) for 8 h at 37°C. Next, the solution was filtered through a 200-mesh filter and centrifuged. Chondrocytes were isolated and cultured in Dulbecco's Modified Eagle's Medium (DMEM) (Hyclone, Logan City, UT, USA) supplemented with 10% fetal bovine serum (FBS) (Gibco, Grand Island, NY, USA), 1% antibiotics (100 U/mL penicillin and 100 U/mL streptomycin; Gibco, Grand Island, NY, USA) at 37°C and 5% CO_2. The medium was changed every 48 h.

Identification of rat chondrocytes: Primary chondrocytes were identified using 1% Alcian blue and toluidine blue (T-B) (Sigma-Aldrich; Merck KGaa) staining for 2 h at room temperature (25°C). Second passage (P2) primary chondrocytes were used for subsequent experiments.

Chondrocyte sheet formation: Chondrocyte sheets were prepared as previously reported [16]. Briefly, P2 chondrocytes were collected and seeded into 6-well plates at 1×10^7 cells/well. High-density seeded chondrocytes were cultured in chondrogenic medium (DMEM supplemented with 40 ng/mL dexamethasone (Sigma-Aldrich, St. Louis, MO, USA), 10 ng/mL transforming growth factor beta-1 (TGF-β1; R&D Systems Inc. Minneapolis, MN, USA), 100 ng/mL insulin-like growth factor 1 (IGF-I' R&D Systems Inc. Minneapolis, MN, USA) for 4 weeks until chondrocyte sheets were formed. The chondrocytes secreted extracellular matrix (ECM) and formed a chondrocyte sheet, which could be detached from the culture dish bottom with tweezers.

Structural observation of the chondrocyte sheets: The chondrocytes sheets were washed three times with phosphate buffer saline (PBS) and then fixed with glutaraldehyde (2.5%) for 2 h at 4°C. Next, the specimens were extensively rinsed with PBS, dehydrated using ethanol gradients, and lyophilized. The samples were then coated with platinum and visualized using scanning electron microscopy (SEM).

In vivo implantation of the chondrocyte sheets

Tissue expansion model: Twelve male Sprague-Dawley rats (body weight 249-312 g; 8 weeks old) were obtained from the Shanghai Jiao Tong University School of Medicine Experimental Animal Center, China. Rats were randomly divided into 4-week (n=6) and 12-week (n=6) groups. Customized rectangular expanders (3.5×2.5×2 cm; Guangzhou Wanhe Medical Instrument Co. Ltd., Guangzhou, China)

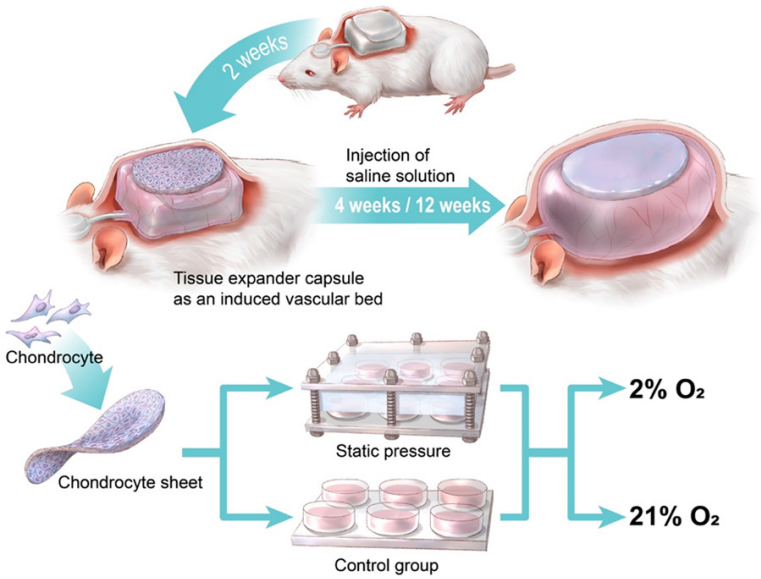

Figure 1. A schematic diagram of the study.

with a volume of 20 ml and a thickened silicone sheet (3.5×2.5×0.1 cm) on top were implanted into each rat. All animals were anesthetized using isoflurane inhalation and surgical procedures were performed in a sterile environment. The expander was implanted deep into the panniculus carnosus on the back of the rats through a 2-cm incision parallel to the spine, and the injection port was placed subcutaneously on the head. Normal saline solution (20 mL) was then injected into the expander intraoperatively to maintain the shape and location of the expander, and to eliminate the dead space.

Implantation of the chondrocyte sheets: After 14 days, a capsule was formed, significantly reducing the possibility of expander displacement. Next, chondrocyte sheets were transplanted on top of the expander capsule. Subsequent inflation was performed every week using 3 mL of saline solution each time. During the inflation process, if serious complications such as expander rupture or flap necrosis occurred, the affected rat was excluded from the study. The animals were then euthanized with high-dose anesthesia either 4 or 12 weeks after transplantation. The detailed process is illustrated in **Figure 1**. On day 31, severe skin necrosis was observed on the expanded skin in one rat of the 4-week group; meanwhile, on day 43, one expander was ruptured in one rat of the 12-week group; these rats were excluded from the study. No other complications occurred during the inflation process.

Histology

At either 4- or 12-week time point, samples were dissected out and analyzed histologically. After gross observation, the samples were fixed in 4% paraformaldehyde for 24 h, dehydrated using graded alcohols, and embedded in paraffin. The embedded samples were sectioned perpendicularly to the surface of the implants into 5-μm-thick sections and then stained with hematoxylin and eosin (H&E), toluidine blue (T-B), or Safranin O/Fast Green (S-F).

Immunohistochemistry and immunofluorescence

Immunohistochemistry was performed as previously described [17, 18]. Briefly, dewaxed sections were washed in PBS and endogenous peroxidase activity was quenched using 2% (v/v) hydrogen peroxide for 5 min. Antigen retrieval was performed by incubating the samples in sodium citrate buffer for 30 min. The sections were washed twice in PBS, blocked with 1.5% goat serum for 30 min at room temperature, and then incubated with primary antibodies (COL II or COL X Abcam, Cambridge, UK) overnight at 4°C. Next, sections were incubated with a peroxidase-conjugated secondary antibody, visualized with a 3,3-diaminobenzidine solution (DAB Substrate Kit, Burlingame, CA, USA), and counter-stained with hematoxylin.

After deparaffinization and rehydration, the tissue sections were incubated with primary antibody (COL II Abcam, Cambridge, UK) overnight at 4°C, following which a fluorescein isothiocyanate-conjugated secondary antibody was added. The nuclei were counterstained with 0.1 mg/mL of 4',6-diamidino-2-phenylindole. Stained sections were then scanned and viewed.

Effect of mechanical forces and hypoxic conditions on cultured chondrocyte sheets in vitro

Application of static pressure: Chondrocytes were cultured on the flexible surface of the Bioflex 6-well plates (Flexcell International Corp, McKeesport, PA, USA) and then subjected to elongation. Static pressure was applied to the chondrocyte sheet using an in-house-designed pressure device. The device was composed of two acrylic plates connected with eight screws. Six cylindrical columns were placed on the bottom plate for support, and the screws were tightened after the top plate was covered. This device provided static pressure with 20% elongation of the flexible surface.

Hypoxia: Once formed, chondrocyte sheets were cultured under either normoxic conditions (21% O_2, 74% N_2, 5% CO_2, saturated humidity and 37°C) or hypoxic conditions (2% O_2, 94% N_2, 5% CO_2, saturated humidity and 37°C) for 14 days. The four culture conditions were abbreviated as follows: H, chondrocyte sheet, hypoxic conditions; P, chondrocyte sheet with static pressure, normoxic conditions; HP, chondrocyte sheet with static pressure, hypoxic conditions; Control, chondrocyte sheet, normoxic conditions.

Western blotting

Western blotting was performed as previously described [19]. Primary antibodies against SOX9 (1:1,000, AF6330, Affinity Biosciences, OH, USA), collagen II (1:1,000, AF0135, Affinity Biosciences, OH, USA), aggrecan (1:1,000, DF7561, Affinity Biosciences, OH, USA), HIF-1α (1:1,000, #14179, Cell Signaling Technology, Danvers, MA, USA), and β-actin (1:1,000, ab8226, Abcam, Cambridge, MA, USA) were used.

Isolation of total RNA, reverse transcription, and quantitative real-time PCR (qRT-PCR)

The isolation of total RNA and reverse transcription were performed as previously described [20]. Briefly, total RNA was isolated using TRIZOL reagent (Ambion) and purified using the RNeasy mini kit (QIAGEN, Valencia, CA, USA). The total RNA was then reverse-transcribed using the Prime Script RT reagent Kit with gDNA Eraser (TaKaRa Code: DRR047A). The sequences of primers for qRT-PCR were as follows (5'-3'): GAPDH: forward, GCAAGTTCAACGGCACAG, reverse, CCAGTAGACTCCACGACAT; Aggrecan: forward, GATAGCCACTGCTGATACA, reverse, CCACTCTTGCCTACCTTC; Col II: forward, GGCGTGAGGTAGAAAAGG, reverse, ATGGTAGAGCGGAACAGG; Sox-9: forward, TTCCAGTCTTCTCACCATT, reverse, AAACTTCATAGCCCTTCTTC; and HIF-1α: forward, AAGTCTAGGGATGCAGCAC, reverse CCAGATCACCAGCATCTAG. The analysis was performed using the Step One Plus PCR system (Applied Biosystems). The amount of target cDNA relative to GAPDH was calculated using the $2^{-\Delta\Delta Ct}$ method. The relative expression of the target gene was then compared to the control group. Each experiment was performed in triplicate and mean values were calculated.

Statistical analysis

All experiments were conducted in triplicate. Data are presented as the mean ± standard deviation. Statistical analyses were conducted using one-way analysis of variance (ANOVA), followed by Tukey's post hoc test using the GraphPad Prism software (GraphPad Software Inc., USA). The level of significance was set at $P<0.05$.

Results

In vitro characterization of chondrocyte sheets

To confirm the presence of chondrocytes in our cultures, cells were stained with T-B and Alcian blue and viewed under a light microscope. Isolated chondrocytes were polygonal in shape with regular dimensions (**Figure 2A-C**). The chondrocyte sheets were formed after 4 weeks (**Figure 2D**), as demonstrated by dense cell distribution. These chondrocyte sheets could be completely detached from the dish bottom using tweezers (**Figure 2E**). SEM images showed abundant overlaying cells, as well as the presence of secreted ECM (**Figure 2F**).

In vivo implantation of chondrocyte sheets

The custom-designed rectangular expanders were coated with thickened silicone sheets on the top surface (**Figure 3A**). To induce vascularized capsule tissue formation, the expanders were inflated using saline solution (**Figure 3B**). After 14 days, the capsule was formed, and

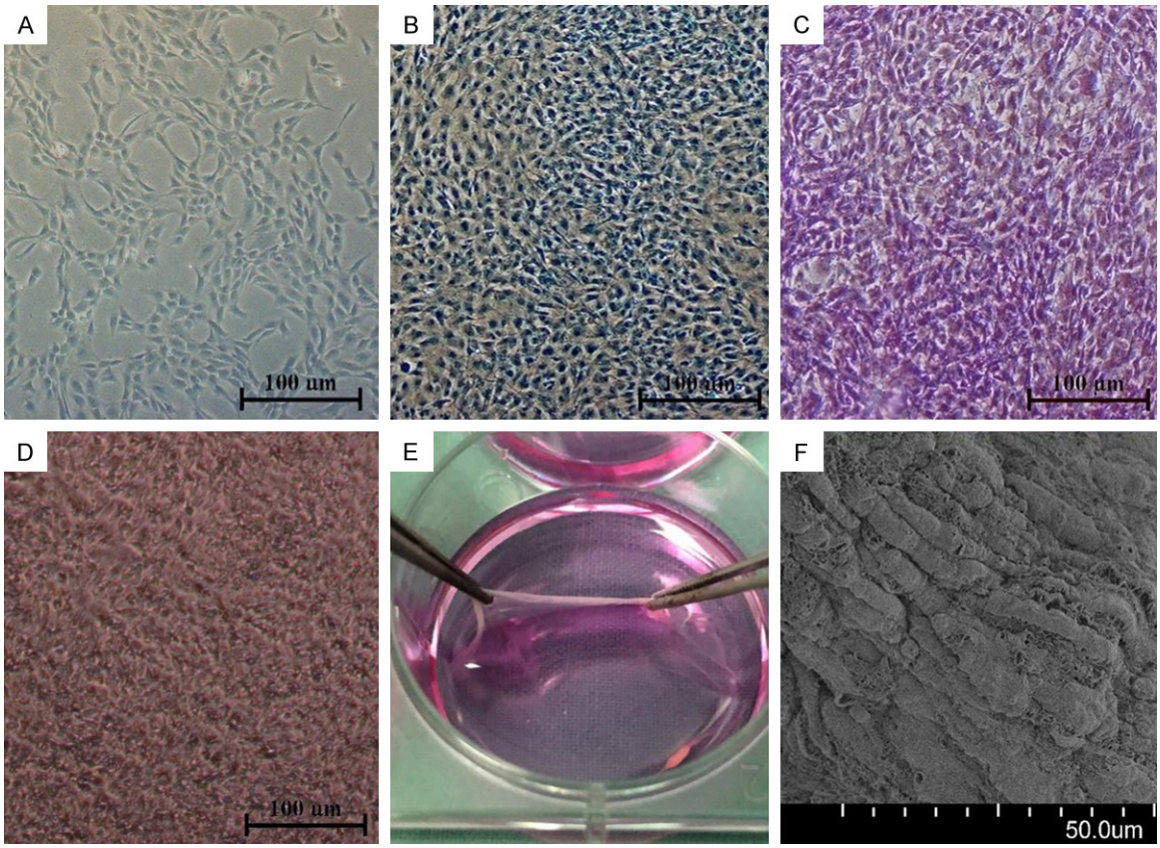

Figure 2. Characterization of chondrocytes and chondrocyte sheets. A-C. Light microscopic images of chondrocyte cultures. Representative images are shown. A. P2 chondrocytes, scale bar: 100 μm. B, C. P2 chondrocyte cultures stained with Alcian blue and toluidine blue, scale bar: 100 μm. D-F. Chondrocyte sheets, representative images are shown. D. Light microscopic images of chondrocyte sheets, scale bar: 100 μm. E. The detachment of chondrocyte sheets after 4 weeks in culture. F. SEM image of chondrocyte sheets, scale bar: 50 μm.

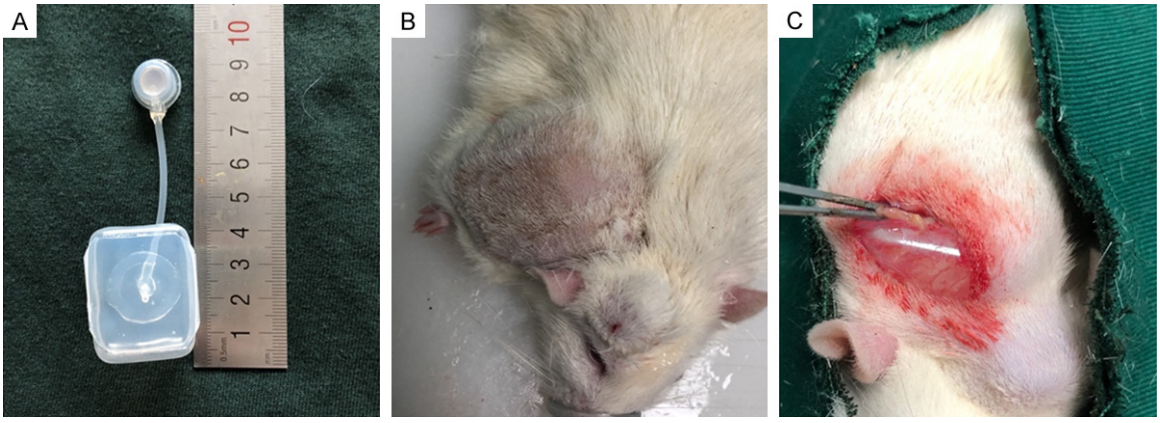

Figure 3. Implantation of the chondrocyte sheets. A. The representative image of a customized rectangular expander used in this study. The expander was coated with a thickened silicone sheet on the top. B. The representative image of an expander inflated with saline solution to induce vascularized capsule tissue formation. C. Representative image of a chondrocyte sheet transplanted onto the expander capsule.

chondrocyte sheets were transplanted onto the expander capsule (**Figure 3C**).

Four and 12 weeks post transplantation of chondrocyte sheets onto the expander cap-

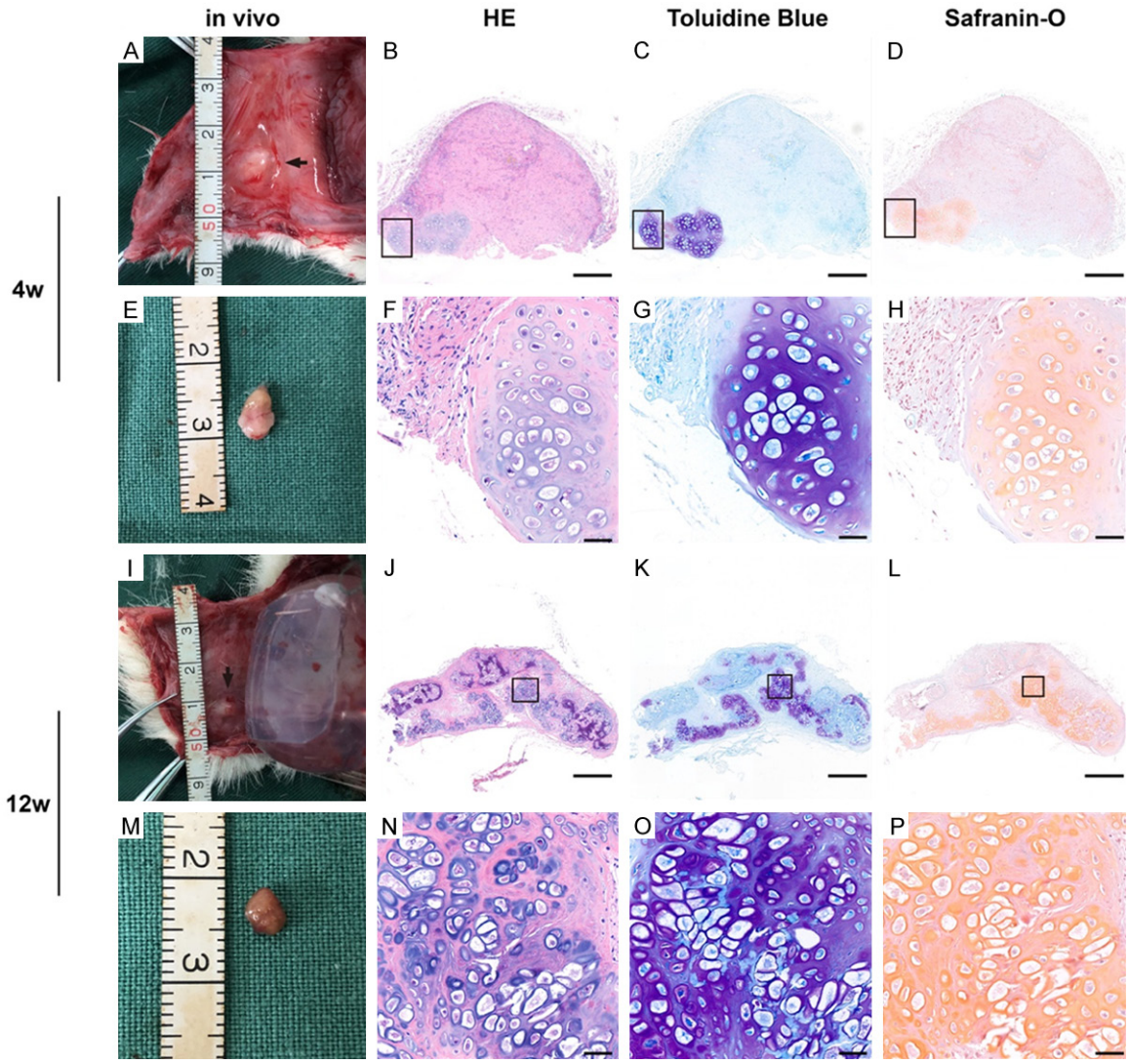

Figure 4. *In vivo* cartilage regeneration, using cell sheets, and characterization of cartilage formation by chondrocyte sheets. (A, I) Gross appearance of cell sheets in expander capsule after 4 and 12 weeks of transplantation, respectively. The black arrows indicate the cartilage tissue. (E, M) Gross appearance of *ex vivo* cartilage tissue after 4 and 12 weeks, respectively. (B, F, J, N) H&E staining of the cartilage-like tissue with cartilage lacuna, at 4 and 12 weeks. (C, G, K, O) Toluidine blue (T-B) staining showing the formation of cartilage-like tissue at 4 and 12 weeks. (D, H, L, P) Safranin O (S-F) staining showing the formation of cartilage-like tissue at 4 and 12 weeks. Original magnification: 40×, scale bar: 500 μm (B, C, J-L); zoomed-in square magnification: 400×, scale bar: 50 μm (F-H, N-P).

sule, implants were removed, and histological and immunohistochemical assays were performed. The gross evaluation of the samples demonstrated the formation of white and glossy neocartilage tissue in both groups *in vivo* (**Figure 4A**, **4I**). All constructs were surrounded by fibrous tissue, which could be easily removed (**Figure 4E**, **4M**). By week 4, chondrocytes were visible within typical chondrocyte lacunae and surrounded by abundant cartilaginous matrix, which had morphological characteristics similar to those of naive cartilage (**Figure 4B-D**, **4F-H**). Meanwhile, by 12 weeks, histological staining demonstrated significantly increased contiguous cartilage matrix deposition compared to 4 weeks. The new tissue showed intense T-B and S-F staining consistent with the cartilage-specific matrix deposition and typical histological structures (**Figure 4J-L**, **4N-P**). Immunohistochemistry confirmed strong COL2A1 expression at both time points, with larger COL2A1 deposits in the

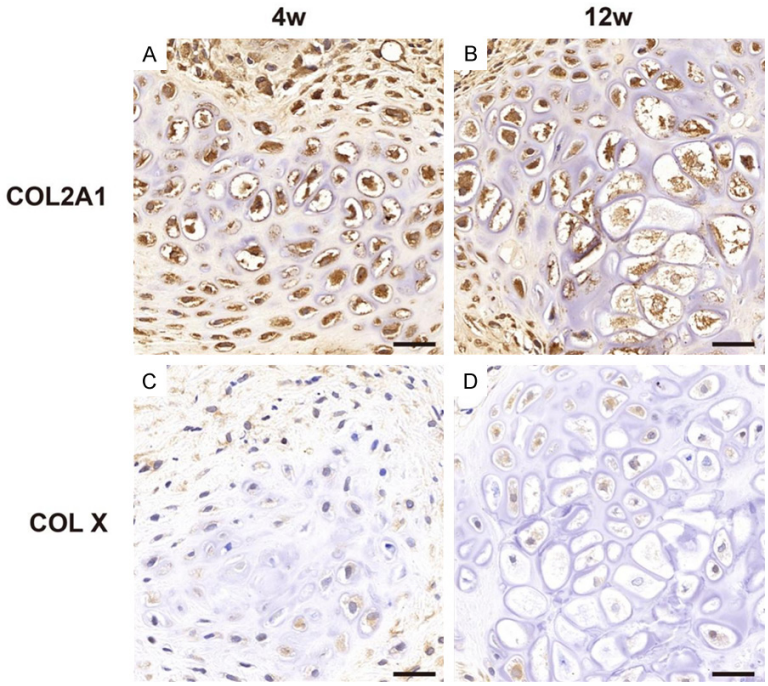

Figure 5. Immunohistochemistry of cartilage tissue formed by chondrocyte sheets *in vivo*. A, B. Collagen II (COL II) staining of the tissues at 4 and 12 weeks. Scale bar: 50 μm. C, D. Collagen X (COL X) staining of the tissues at 4 and 12 weeks, representative images. COL X is a marker of hypertrophy, suggesting that several chondrocytes exhibited a hypertrophic phenotype at 12-week time point. Scale bar: 50 μm.

12-week group (**Figure 5A**, **5B**). Tissue sections were also positive for COL X, especially in the 12-week group (**Figure 5C**, **5D**).

Effect of mechanical forces and hypoxic conditions on cultured chondrocyte sheets in vitro

To investigate the effect of mechanical forces and hypoxia, chondrocyte sheets were cultured *in vitro*. After 2 weeks of culture, no apparent differences between the four different conditions were observed (**Figure 6A-D**). The SEM images showed abundant overlaying cells, as well as secreted rich gelatinous ECM, giving the sheets a wave-like appearance in all groups (**Figure 6E-H**).

Histological examination of all groups showed that chondrocyte sheets maintained their cartilage-like appearance (**Figure 7**). Interestingly, the chondrocyte sheets in the H group appeared to be thicker than those in other groups, as demonstrated by H&E staining (**Figure 7C**, **7G**). T-B and S-F staining confirmed the deposition of cartilage-like ECM (**Figure 7Q-X**), with high staining intensity levels in the H group and low levels in the P group compared with those in other groups, while the tissue morphology of the HP group appeared to be similar to the control group.

Next, we evaluated the expression of chondrocyte-specific COL2A1 in chondrocyte sheets using immunofluorescence (**Figure 7Y**). Fluorescence microscopy demonstrated that all groups were positive for COL2A1. Furthermore, the levels of COL2A1 in chondrocytes cultured under hypoxic conditions (H group) appeared to be higher compared to all other groups.

Western blot analysis

To confirm our immunohistochemistry observations, we performed western blot analysis (**Figure 8A**), which showed a decrease in collagen II protein levels in the P group, while the levels of HIF-1α was higher in H and HP groups compared to the control group.

Gene expression (real-time PCR)

To further verify our histology and immunostaining results, the expression levels of chondrocyte-specific genes, such as *Aggrecan*, *COL II*, *Sox-9*, and *HIF-1α*, was analyzed in chondrocyte sheets. Our results demonstrated that chondrocyte sheets exposed to static pressure (P group) had significantly lower levels of *Aggrecan*, *COL II*, and *Sox-9* compared with those in the hypoxia (H), HP, and control groups ($P<0.05$) (**Figure 8B-D**). There were no significant differences in *Aggrecan* and *COL II* expression between H and HP groups and the control group (**Figure 8B**, **8C**). At the same time, the H group showed higher *Sox-9* gene expression than did the control group ($P<0.05$) (**Figure 8D**), while Sox-9 levels in the HP group, although significantly higher than those in the P group, were similar to those in the control group ($P>0.05$). Finally, the expression of *HIF-1α* in chondrocyte sheets was increased in response to hypoxic conditions in both H and HP groups

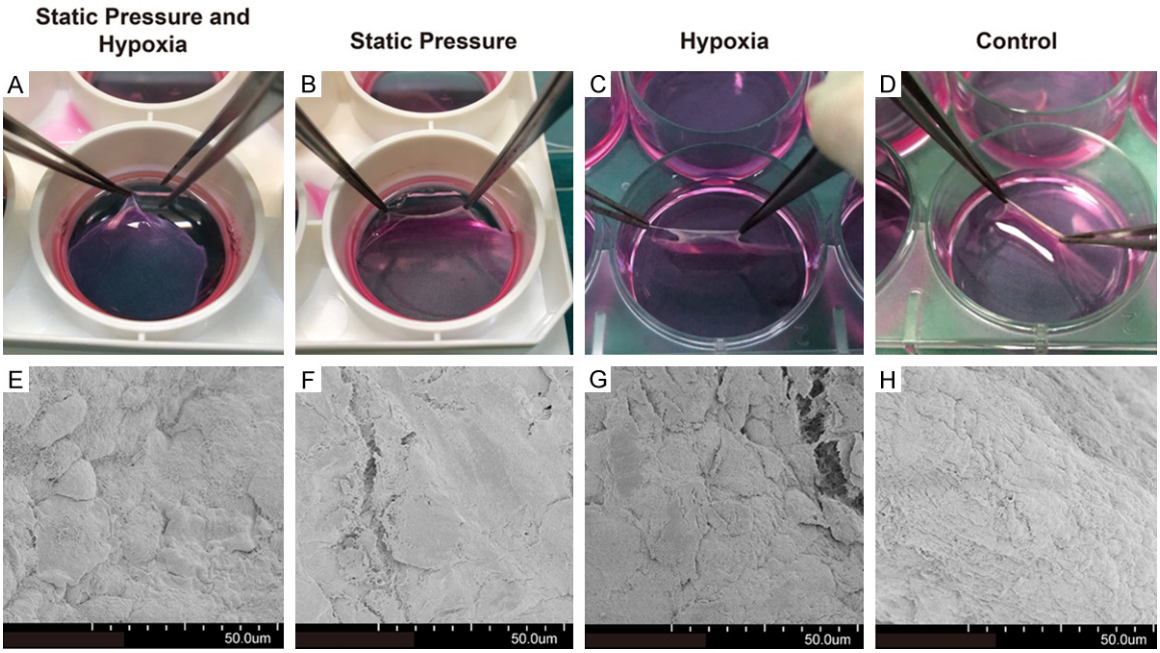

Figure 6. Characterization of chondrocyte sheets cultured *in vitro* under static pressure and hypoxic conditions. A-D. The chondrocyte sheets detached from the plate surface. E-H. SEM images of chondrocyte sheets cultured under different conditions. Scale bar: 50 μm.

compared with that in the control and P groups ($P<0.05$) (**Figure 8E**).

Discussion

The reconstruction of complex defects involves multi-steps of surgeries, and multiple tissue flaps are often required. For the simultaneous restoration of several absent tissue types, the prelamination of expanded flaps is commonly used to repair these defects [21]. Mutaf *et al*. [7] have indicated that skin expansion creates a favorable environment for cartilage grafting and have reported the growth potential of the cartilage framework. Meanwhile, Erkin *et al*. [21] have developed a new model of flap prelamination in rats using xenogenic and autogenic tissues, including autologous fascia, muscle, bone, cartilage, grafts, and acellular human dermal matrix, and have suggested that these kinds of free flap prefabrications could reduce autogenous tissue sacrifice.

Tan *et al*. [22] have suggested that flap prelamination has significant potential in plastic surgery since bridges the gap between conventional reconstructive surgery and tissue engineering. By applying this technique, tissues could be preassembled to form precise composites that would accommodate the different types of defects. For example, Staudenmaier *et al*. [9] performed flap prelamination using tissue-engineered cartilage by implanting a vessel loop under a random-pattern abdominal skin flap. The tissue-engineered cartilage constructs were then prepared by isolating chondrocytes from auricular biopsies, seeding the cells onto hyaluronic-acid derivative, and then culturing for 2 weeks. The authors also reported that the tissue-engineered constructs remained stable in size and were similar to hyaline cartilage. Von Bomhard *et al*. [23] reported an autologous model by combining prefabricated skin flaps with the implantation of vascular pedicle and *in vitro* cultured chondrocyte bioconstructs in order to manufacture functional three-dimensional cartilage grafts.

Both Staudenmaier [9] and von Bomhard [23] used scaffold materials since they are essential in tissue engineering [24, 25]. Unfortunately, scaffold materials, either synthetic polymers or natural, have numerous shortcomings, hence the tissue formed is inferior to the native cartilage, as demonstrated by their morphology and function. The recently developed cell-sheet technique presents a possible solution to overcome these

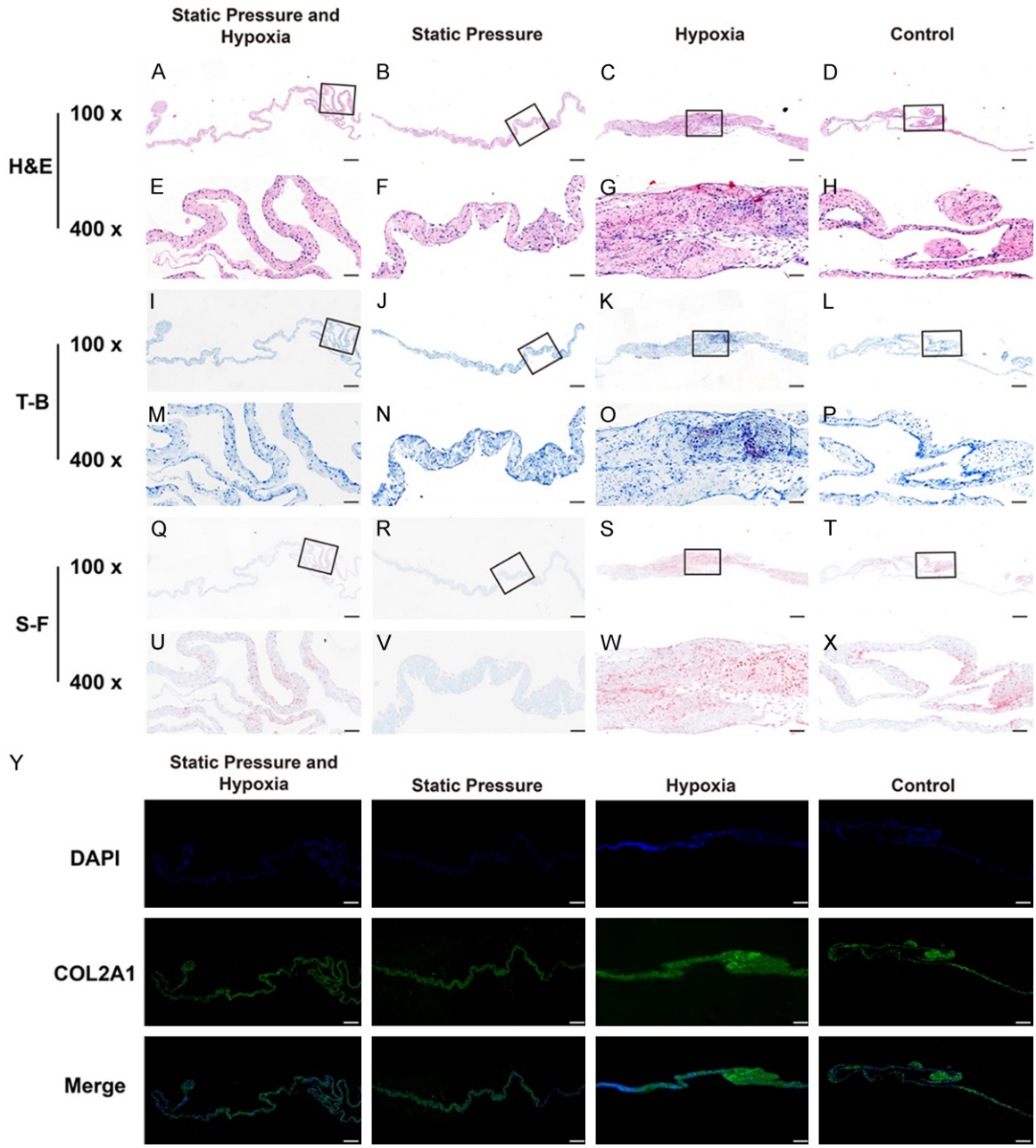

Figure 7. Histological analysis and COL2A1 immunofluorescent staining of chondrocyte sheets cultured *in vitro* under static pressure and hypoxic conditions. (A-H) H&E staining, (I-P) toluidine blue (T-B) staining, and (Q-X) Safranin O/Fast green (S-F) staining, (Y) COL2A1 immunofluorescent staining (green), nuclei were counterstained with DAPI (blue). Original magnification: 100×, scale bar: 200 μm (A-D, I-L, Q-T, Y); zoomed-in square magnification 400×, scale bar: 50 μm (E-H, M-P, U-X).

shortcomings since it could be used for cartilage regeneration in the absence of a scaffold [10, 11, 26]. The chondrocyte sheet consists of cells and ECM, where it provides a structural and nutritive microenvironment and promotes cell adhesion, growth, and tissue regeneration *in vivo* [27]. To regenerate cartilage, it has been previously suggested that, due to the limited number of chondrocytes, bone marrow stromal cells first differentiate into chondrocytes and then form chondrocyte sheets [28-30]. Yanaga *et al*. [31] confirmed the redifferentiation of expanding chondrocytes using a multiple layer culturing system. Furthermore, Liao *et al*. [32]

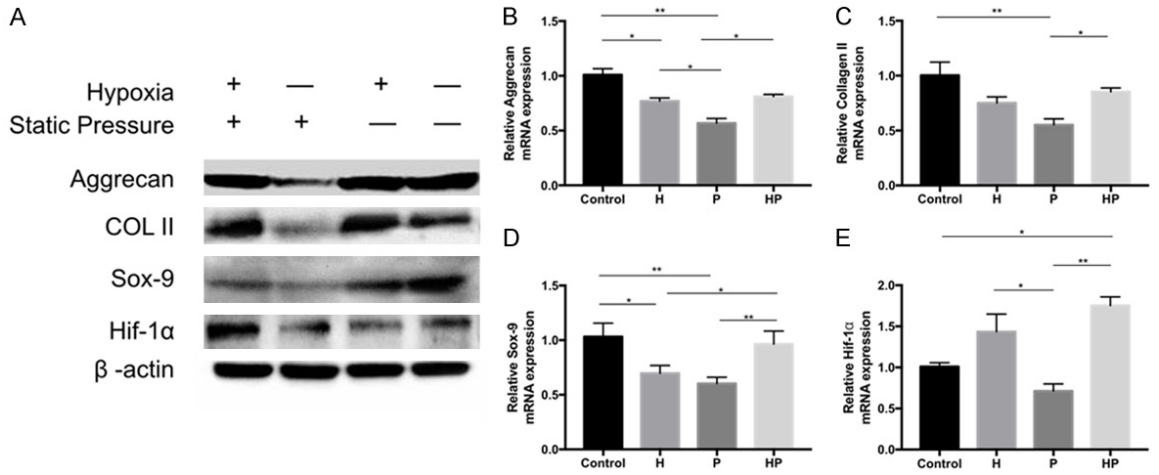

Figure 8. Evaluation of protein expression and cartilage-related genes in the chondrocyte sheets cultured *in vitro* under static pressure and hypoxic conditions. (A) Protein expression of Aggrecan, COL II, Sox-9, and HIF-1α as determined using western blotting; β-actin was used as a loading control. The expression of Aggrecan (B), COL II (C), Sox-9 (D) and HIF1-α (E) genes was determined using real-time PCR. GAPDH was used as a housekeeping gene. Data are presented as the mean ± standard deviation (n=3), *P<0.05.

demonstrated that a stable chondrocyte sheet could be established by seeding expanded chondrocytes (passage 2 or 3) at high density without the primary chondrocyte sheet. Here, we used chondrocyte sheets to regenerate cartilage. High-density chondrocyte cultures promoted chondrocyte proliferation and enhanced ECM synthesis: abundant cells secreted a large amount of ECM, linking cells to form a durable and stable cell sheet. In addition, our *in vivo* results suggested that the continuous inflation of tissue expander (for up to 12 weeks) induced chondrocyte hypertrophy, which is essential for endochondral ossification.

Previous studies have suggested that during cartilage flap prelamination, the tissues are assembled in a vascular loop or a vascular bundle, and that tissue vascularization takes approximately 3 weeks [9, 33-37]. In tissue engineering, the expander capsule induction technique provides several advantages for vascularization. The tissue expander creates a spherical capsule pouch, inducing foreign body reaction, thereby promoting neovascularization inside the tissue. This induction technique is a safe and reliable method as demonstrated by consistently viable capsule flap post transposition [38, 39]. Jia *et al*. [40] showed that the tissue expander capsule served as an axial vascular bed to create vascularized engineered tissue with its own vessels using cell sheet engineering. In our study, we used expanded capsule tissue as a vascular bed for pre-vascularization.

Since cartilage tissues lack vasculature, chondrocytes reside in a hypoxic microenvironment, where oxygen levels range from 6% in the superficial zone to 1% in the deep zone, resulting in physiological chronic hypoxia [41, 42]. Hypoxic conditions have been shown to be beneficial for the maintenance of chondrogenic phenotype [43] and for the induction of cartilage-specific marker re-expression in chondrocytes [44, 45]. Kobuko *et al*. [46] compared cells cultured in 21% oxygen *vs*. 2% oxygen, the oxygen level found in deep cartilage, and found that layered chondrocyte sheets rich in ECM were generated sooner in the 2% oxygen group. Here, our results showed that, compared to the 21% oxygen condition, chondrocyte sheets cultured in 2% oxygen maintained their chondrogenic phenotype, and the expression levels of Sox-9 and HIF-1α were increased. Sox-9, the transcription factor essential for chondrocyte differentiation and cartilage formation, marks the earliest stage of chondrocyte lineage [47]. Presumably, this led to elevated expression of *ACAN* and collagen II, the extracellular matrix genes and transcription targets of SOX9 [46]. Markway *et al*. [48] have reported that hypoxia induces the expression of collagen II and proteoglycan through

HIF-1α, while promoting the anabolic metabolism of chondrocytes. Our results indicate that hypoxia increased the expression of cartilage-specific markers in chondrocytes and maintained the chondrogenic phenotype.

Several studies have shown that pressure is another essential factor necessary to maintain the normal function of articular cartilage [49, 50]. While the physiological pressure levels contribute to the maintenance of cartilage health, abnormal pressure levels lead to irreparable cartilage damage. Conversely, other studies have suggested that static pressure has detrimental effects on chondrocyte anabolism by reducing the synthesis of ECM components, accelerating the osteogenic differentiation of chondrocytes, and inducing chondrocyte apoptosis [51-53]. The tissue expander provides mechanical static pressure following inflation. In our study, we designed a customized tissue expander coated with a thickened silicone sheet, resulting in the generation of consistent pressure on the surface during inflation. *In vitro*, we used a pressure device designed in-house that provided 20% elongation of the chondrocyte sheet on the flexible surface, the elongation similar to the tissue expander following regular inflation. The results showed that static pressure did not promote cartilage formation as demonstrated by the downregulation of aggrecan, collagen II, and Sox-9 expression levels. However, the combination of mechanical stress and hypoxia simulated chondrocyte sheet formation and the increased expression of cartilage-specific genes, which contributed to the maintenance of the chondrogenic phenotype. Hence, our results suggest that these conditions mimicked the hypoxic environment, where the ECM of cartilage is produced and maintained. In chondrocytes, HIF-1α is involved in anaerobic metabolism and inhibits cell apoptosis in response to hypoxia [54], further supporting our observations of increased HIF-1α levels in chondrocyte sheets cultured under hypoxic conditions.

This study has some limitations. First, the shape of the cartilage of the prelaminated flap was spheroid, since we did not flatten the chondrocyte sheet during the surgery. Liao *et al*. [32] used an ear-shaped titanium alloy scaffold and covered it using a chondrocyte sheet to prelaminate the ear-shaped engineered cartilage tissue. We will modify the shape of the cartilage tissue in our future studies. Second, since observational endpoints were 4 and 12 weeks, no investigation on the long-term continuous expansion following chondrocyte sheet implantation *in vivo* was conducted, therefore, the correlation between chondrocyte sheet implantation and the period of expansion should be further explored. Finally, we did not evaluate the elasticity of the generated cartilage *ex vivo*. The properties of engineered tissues, including cartilage development and tissue interaction, were investigated only using qualitative histochemical methods. However, the mechanistic studies evaluating the activation of signaling pathways are currently underway. All these limitations will be addressed in our future studies.

In summary, our results indicate that, in a tissue expansion model, it is possible to prelaminate chondrocutaneous flap by implanting a chondrocyte sheet above the expander capsule. The development of a tissue similar to hyaline cartilage was confirmed by the expression of cartilage-specific aggrecan and collagen II. The tissue expansion technique provided mechanical static pressure and the hypoxic environment necessary for the maintenance of a chondrogenic phenotype. Furthermore, our study demonstrated that tissue expansion promoted chondrocyte cell sheets to form tissue-engineered cartilage, while in vitro mechanical forces and hypoxic conditions allowed for chondrocyte cell sheets to retain their chondrogenic phenotype.

Acknowledgements

This research was funded by the National Natural Science Foundation of China, Grant number 81772324 and 81801929.

Disclosure of conflict of interest

None.

Address correspondence to: Ke Xue and Kai Liu, Department of Plastic and Reconstructive Surgery, Shanghai Ninth People's Hospital, Shanghai Jiao Tong University School of Medicine, 639 Zhi Zao Ju Road, Shanghai 200011, People's Republic of China. Tel: +86-23271699; E-mail: drkexue@126.com (KX); drkailiu@163.com (KL)

References

[1] Seikaly H, Rieger J, Wolfaardt J, Moysa G, Harris J and Jha N. Functional outcomes after primary oropharyngeal cancer resection and reconstruction with the radial forearm free flap. Laryngoscope 2003; 113: 897-904.

[2] Pribaz JJ, Fine N and Orgill DP. Flap prefabrication in the head and neck: a 10-year experience. Plast Reconstr Surg 1999; 103: 808-820.

[3] Yao ST. Microvascular transplantation of prefabricated free thigh flap. Plast Reconstr Surg 1982; 69: 568-568.

[4] Pribaz JJ and Fine NA. Prelamination: defining the prefabricated flap: a case report and review. Microsurgery 1994; 15: 618-623.

[5] Radovan C. Tissue expansion in soft-tissue reconstruction. Plast Reconstr Surg 1984; 74: 482-492.

[6] Bennett RG and Hirt M. A history of tissue expansion. Concepts, controversies, and complications. J Dermatol Surg Oncol 1993; 19: 1066-1073.

[7] Mutaf M, Celebioglu S and Sensoz O. Growth potential of autogenous cartilage grafts in expanded skin: an experimental study in rabbits. Ann Plast Surg 1994; 32: 126-131.

[8] Geishauser M, Staudenmaier RW and Biemer E. Donor-site morbidity of the segmental rectus abdominis muscle flap. Br J Plast Surg 1998; 51: 603-607.

[9] Staudenmaier R, Hoang TN, Kleinsasser N, Schurr C, Frolich K, Wenzel MM and Aigner J. Flap prefabrication and prelamination with tissue-engineered cartilage. J Reconstr Microsurg 2004; 20: 555-564.

[10] Matsuura K, Ito K, Shiraki N, Kume S, Hagiwara N and Shimizu T. Induced pluripotent stem cell elimination in a cell sheet by methionine-free and 42 degrees c condition for tumor prevention. Tissue Eng Part C Methods 2018; 24: 605-615.

[11] Matsuura K, Utoh R, Nagase K and Okano T. Cell sheet approach for tissue engineering and regenerative medicine. J Control Release 2014; 190: 228-239.

[12] Maitz PK, Pribaz JJ and Hergrueter CA. Impact of tissue expansion on flap prefabrication: an experimental study in rabbits. Microsurgery 1996; 17: 35-40.

[13] Wang X, Li C, Zheng Y, Xia W, Yu Y and Ma X. Bone marrow mesenchymal stem cells increase skin regeneration efficiency in skin and soft tissue expansion. Expert Opin Biol Ther 2012; 12: 1129-1139.

[14] Li H, Huang L, Xie Q, Cai X, Yang C, Wang S and Zhang M. Study on the effects of gradient mechanical pressures on the proliferation, apoptosis, chondrogenesis and hypertrophy of mandibular condylar chondrocytes in vitro. Arch Oral Biol 2017; 73: 186-192.

[15] Li H, Li X, Jing X, Li M, Ren Y, Chen J, Yang C, Wu H and Guo F. Hypoxia promotes maintenance of the chondrogenic phenotype in rat growth plate chondrocytes through the HIF-1 alpha/YAP signaling pathway. Int J Mol Med 2018; 42: 3181-3192.

[16] Li D, Yin Z, Liu Y, Feng S, Liu Y, Lu F, Xu Y, Min P, Hou M, Li K, He A, Zhang W, Liu W, Zhang Y, Zhou G and Cao Y. Regeneration of trachea graft with cartilage support, vascularization, and epithelization. Acta Biomater 2019; 89: 206-216.

[17] Liu K, Zhou GD, Liu W, Zhang WH, Cui L, Liu X, Liu TY and Cao Y. The dependence of in vivo stable ectopic chondrogenesis by human mesenchymal stem cells on chondrogenic differentiation in vitro. Biomaterials 2008; 29: 2183-2192.

[18] Chen Y, Xue K, Zhang X, Zheng Z and Liu K. Exosomes derived from mature chondrocytes facilitate subcutaneous stable ectopic chondrogenesis of cartilage progenitor cells. Stem Cell Res Ther 2018; 9: 318.

[19] Zhang X, Qi L, Chen Y, Xiong Z, Li J, Xu P, Pan Z, Zhang H, Chen Z, Xue K and Liu K. The in vivo chondrogenesis of cartilage stem/progenitor cells from auricular cartilage and the perichondrium. Am J Transl Res 2019; 11: 2855-2865.

[20] Xue K, Xia W, Zhang X, Qi L, Zhou J, Xu P and Liu K. Isolation and identification of stem cells in different subtype of cartilage tissue. Expert Opin Biol Ther 2015; 15: 623-632.

[21] Erkin UR, Kerem M, Tug M, Orbay H and Sensoez O. Prefabrication of a conjoint flap containing xenogenic tissues: a preliminary report on an experimental model. J Craniofac Surg 2007; 18: 1451-1456.

[22] Tan BK, Chen HC, He TM and Song IC. Flap prefabrication-the bridge between conventional flaps and tissue-engineered flaps. Ann Acad Med Singap 2004; 33: 662-666.

[23] von Bomhard A, Veit J, Bermueller C, Rotter N, Staudenmaier R, Storck K and Hoang Nguyen T. Prefabrication of 3D cartilage contructs: towards a tissue engineered auricle-a model tested in rabbits. PLoS One 2013; 8: e71667.

[24] Langer R and Vacanti JP. Tissue engineering. Science 1993; 260: 920-926.

[25] Bhardwaj N, Devi D and Mandal BB. Tissue-engineered cartilage: the crossroads of biomaterials, cells and stimulating factors. Macromol Biosci 2015; 15: 153-182.

[26] Lu Y, Zhang W, Wang J, Yang G, Yin S, Tang T, Yu C and Jiang X. Recent advances in cell sheet technology for bone and cartilage regenera-

tion: from preparation to application. Int J Oral Sci 2019; 11: 17.
[27] Yanaga H, Imai K, Koga M and Yanaga K. Cell-engineered human elastic chondrocytes regenerate natural scaffold in vitro and neocartilage with neoperichondrium in the human body post-transplantation. Tissue Eng Part A 2012; 18: 2020-2029.
[28] Long T, Zhu Z, Awad HA, Schwarz EM, Hilton MJ and Dong Y. The effect of mesenchymal stem cell sheets on structural allograft healing of critical sized femoral defects in mice. Biomaterials 2014; 35: 2752-2759.
[29] Sato Y, Wakitani S and Takagi M. Xeno-free and shrinkage-free preparation of scaffold-free cartilage-like disc-shaped cell sheet using human bone marrow mesenchymal stem cells. J Biosci Bioeng 2013; 116: 734-739.
[30] Li D, Zhu L, Liu Y, Yin Z, Liu Y, Liu F, He A, Feng S, Zhang Y, Zhang Z, Zhang W, Liu W, Cao Y and Zhou G. Stable subcutaneous cartilage regeneration of bone marrow stromal cells directed by chondrocyte sheet. Acta Biomater 2017; 54: 321-332.
[31] Yanaga H, Imai K, Fujimoto T and Yanaga K. Generating ears from cultured autologous auricular chondrocytes by using two-stage implantation in treatment of microtia. Plast Reconstr Surg 2009; 124: 817-825.
[32] Liao HT, Zheng R, Liu W, Zhang WJ, Cao Y and Zhou G. Prefabricated, ear-shaped cartilage tissue engineering by scaffold-free porcine chondrocyte membrane. Plast Reconstr Surg 2015; 135: 313e-321e.
[33] Higgins JP, Borumandi F, Buerger HK, Benlidayi ME, Vasilyeva A, Sencar L, Polat S and Gaggl AJ. Nonvascularized cartilage grafts versus vascularized cartilage flaps: comparison of cartilage quality 6 months after transfer. J Hand Surg Am 2018; 43: 188.e1-188.e8.
[34] Demirtas Y, Engin MS, Aslan O, Ayas B and Karacalar A. The effect of "minimally invasive transfer of angiosomes" on vascularization of prefabricated/prelaminated tissues. Ann Plast Surg 2010; 64: 491-495.
[35] Mandlik V, Kehrer A, Jiga L, Hoinoiu B, Ionac M, Jung F, Staudenmaier R and Prantl L. Prefabrication and free transfer of a tissue engineered composite flap-an experimental model in the rat. Clin Hemorheol Microcirc 2016; 64: 319-331.
[36] Hirase Y, Valauri FA and Buncke HJ. Neovascularized free cutaneous cartilage flap transfer with microsurgical anastomosis: an experimental model in the rabbit. Ann Plast Surg 1988; 21: 342-347.
[37] Tsagarakis M, Spyropoulou GA, Lykoudis E, Papalois A, Tsimponis A, Fragia C, Iconomou T and Papadopoulos O. The use of vascularized fascia as carrier in cases of prelaminated fasciocartilaginous and osseofascial flaps. J Reconstr Microsurg 2016; 32: 301-308.
[38] Schoeller T, Neumeister MW, Huemer GM, Russell RC, Lille S, Otto-Schoeller A and Wechselberger G. Capsule induction technique in a rat model for bladder wall replacement: an overview. Biomaterials 2004; 25: 1663-1673.
[39] Guo HL, Peng XF, Bao XQ, Wang L, Jia ZM, Huang YC, Zhou JM, Xie H and Chen F. Bladder reconstruction using autologous smooth muscle cell sheets grafted on a pre-vascularized capsule. Theranostics 2020; 10: 10378-10393.
[40] Jia Z, Guo H, Xie H, Zhou J, Wang Y, Bao X, Huang Y and Chen F. Construction of pedicled smooth muscle tissues by combining the capsule tissue and cell sheet engineering. Cell Transplant 2019; 28: 328-342.
[41] Schipani E, Ryan HE, Didrickson S, Kobayashi T, Knight M and Johnson RS. Hypoxia in cartilage: HIF-1 alpha is essential for chondrocyte growth arrest and survival. Genes Dev 2001; 15: 2865-2876.
[42] Brucker PU, Izzo NJ and Chu CR. Tonic activation of hypoxia-inducible factor 1 alpha in avascular articular cartilage and implications for metabolic homeostasis. Arthritis Rheum 2005; 52: 3181-3191.
[43] Schrobback K, Klein TJ, Crawford R, Upton Z, Malda J and Leavesley DI. Effects of oxygen and culture system on in vitro propagation and redifferentiation of osteoarthritic human articular chondrocytes. Cell Tissue Res 2012; 347: 649-663.
[44] Mhanna R, Oeztuerk E, Schlink P and Zenobi-Wong M. Probing the microenvironmental conditions for induction of superficial zone protein expression. Osteoarthritis Cartilage 2013; 21: 1924-1932.
[45] Mennan C, Garcia J, McCarthy H, Owen S, Perry J, Wright K, Banerjee R, Richardson JB and Roberts S. Human articular chondrocytes retain their phenotype in sustained hypoxia while normoxia promotes their immunomodulatory potential. Cartilage 2019; 10: 467-479.
[46] Kokubo M, Sato M, Yamato M, Mitani G, Uchiyama Y, Mochida J and Okano T. Characterization of layered chondrocyte sheets created in a co-culture system with synoviocytes in a hypoxic environment. J Tissue Eng Regen Med 2017; 11: 2885-2894.
[47] Bi WM, Deng JM, Zhang ZP, Behringer RR and de Crombrugghe B. Sox9 is required for cartilage formation. Nature Genetics 1999; 22: 85-89.
[48] Markway BD, Cho H and Johnstone B. Hypoxia promotes redifferentiation and suppresses markers of hypertrophy and degeneration in

both healthy and osteoarthritic chondrocytes. Arthritis Res Ther 2013; 15: R92.
[49] Kiviranta I, Jurvelin J, Tammi M, Saamanen AM and Helminen HJ. Weight bearing controls glycosaminoglycan concentration and articular cartilage thickness in the knee joints of young beagle dogs. Arthritis Rheum 1987; 30: 801-809.
[50] Huang L, Cai X, Li H, Xie Q, Zhang M and Yang C. The effects of static pressure on chondrogenic and osteogenic differentiation in condylar chondrocytes from temporomandibular joint. Arch Oral Biol 2015; 60: 622-630.
[51] Cheleschi S, Barbarino M, Gallo I, Tenti S, Bottaro M, Frati E, Giannotti S and Fioravanti A. Hydrostatic pressure regulates oxidative stress through microRNA in human osteoarthritic chondrocytes. Int J Mol Sci 2020; 21: 3653.
[52] Shieh AC and Athanasiou KA. Dynamic compression of single cells. Osteoarthritis Cartilage 2007; 15: 328-334.
[53] Zhang M, Zheng T, Zong M, Kong D, Li X, Xue C, Fu P and Fang J. Sustained static stress-induced chondrocyte apoptosis in the rat cervical vertebral growth plate and its signal transduction mechanisms. Eur J Orthop Surg Traumatol 2014; 24 Suppl 1: 299-304.
[54] Kosyna FK, Nagel M, Kluxen L, Kraushaar K and Depping R. The importin alpha/beta-specific inhibitor Ivermectin affects HIF-dependent hypoxia response pathways. Biol Chem 2015; 396: 1357-1367.